Nonlinear Dyn (2010) 62: 237–251
DOI 10.1007/s11071-010-9714-6

ORIGINAL PAPER

Experimental characterization of nonlinear systems: a real-time evaluation of the analogous Chua's circuit behavior

Ronilson Rocha · Guilherme L.D. Andrucioli · Rene O. Medrano-T

Received: 15 July 2009 / Accepted: 31 March 2010 / Published online: 27 April 2010

Abstract This paper presents an experimental characterization of the behavior of an analogous version of the Chua's circuit. The electronic circuit signals are captured using a data acquisition board (DAQ) and processed using LabVIEW environment. The following aspects of the time series analysis are analyzed: time waveforms, phase portraits, frequency spectra, Poincaré sections, and bifurcation diagram. The circuit behavior is experimentally mapped with the parameter variations, where are identified equilibrium points, periodic and chaotic attractors, and bifurcations. These analysis techniques are performed in real-time and can be applied to characterize, with precision, several nonlinear systems.

Keywords Chaotic systems · Electronic analogy · Nonlinear dynamics · Data acquisition · Analogous Chua's circuit

R. Rocha (✉) · G.L.D. Andrucioli
Federal University of Ouro Preto—UFOP/EM/DECAT, Campus Morro do Cruzeiro, 35400-000, Ouro Preto, MG, Brazil
e-mail: rocha@em.ufop.br

G.L.D. Andrucioli
e-mail: guilhermeandrucioli@yahoo.com.br

R.O. Medrano-T
University of São Paulo—USP/Institute of Physics, C-P: 66318, 05508-900, São Paulo, SP, Brazil
e-mail: rmedrano@if.usp.br

1 Introduction

Chaotic systems present an unpredictability behavior extremely sensitive to parameters variations and initial conditions, although they are completely described by deterministic laws and nonlinear differential equations without stochastic components. This dynamical behavior has been extensively studied by mathematicians, physicians, engineers, and more recently, specialists in information and social sciences, due to its great potential for commercial and industrial applications in areas such as engineering, informatics, electronics, communication, robotics, chemistry, medicine, biology, epidemiology, management, finance, information processing, etc. [1–3]. One of the most important chaotic systems was created in 1983, an electrical circuit constituted by a network of linear passive elements connected to a nonlinear active component, known as Chua's diode, which standard form is shown in Fig. 1. Since its initial proposal, the Chua's circuit is intensely investigated and has been accepted as paradigm for study of important features of nonlinear systems, once it exhibits a very complex dynamical behavior in spite of its simplicity [4]. It still presents a novel and rich scenario formed by a large variety of homoclinic orbits and bifurcations [5], periodic structures [6], and distinct chaotic attractors [7].

For the experimental point of view, a characterization of dynamical behavior of a nonlinear system only based in computer simulations is not totally reliable, since the simulated model may only describe the sys-

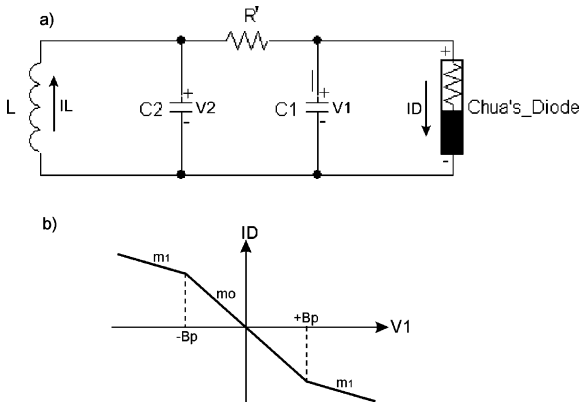

Fig. 1 Schematic Chua's circuit. (**a**) Standard form of the Chua's circuit. (**b**) Characteristic of Chua's diode

tem in an approximate sense. Due to finite precision of the machines and successive approximations, numerical procedures are always subject to round-off errors. Computer simulations are also completely deterministic and do not depend on natural variation of conditions, generating identical solutions when provided with identical initial conditions. Thus, an experimental characterization of a nonlinear system plays a very important role to understand theoretical concepts and it is indispensable for a more rigorous analysis [8]. Any unusual behavior of a dynamical system that is verified during the development of experimental procedures, intentionally or not, can motivate in-depth analysis of underlying mechanisms, generating more appropriate models to explain and predict similar events.

Usually, the analysis of time series produced by the nonlinear system is an important issue to realize its experimental characterization, providing useful information and interpretations concerning to dynamical behaviors [9]. Time-domain waveforms and phase portraits are familiar to most researchers, which can be enough in several situations to identify various dynamical properties of a system. Another technique for experimental analysis of time series is the harmonic decomposition of the measured signal using the Fast Fourier Transform (FFT), obtaining the power spectrum with the harmonics, subharmonics, and ultra-harmonics, which provides an easy way to identify and to capture the signature of nonlinear phenomena. One approach to study nonlinear systems is the exam of a two-dimensional plane that intersects the system trajectories, known as Poincaré section, where it is possible to identify periodic, quasi-periodic and chaotic motions. An usual perspective for a qualitative analysis of the system behavior is the bifurcation diagram, a graphic representation of sampled attractors in a Poincaré section with respect to each value of a chosen system parameter. It provides a nice summary for the transition between different types of motion that can occur when one parameter of the system is varied.

This paper presents an automatized analysis of the experimental behavior of the analogous version of the Chua's circuit proposed by Rocha and Medrano [7] using the LabVIEW, an integrated environment for development of applications related to measurements, tests and control. Although several possibilities can be used to investigate nonlinear phenomena, this work considers methods based in the analysis of times series produced by the circuit, which are captured by a low expensive data acquisition system. The LabVIEW codes for experimental analyses are developed for the simultaneous observation of time waveforms, phase portraits, frequency spectra, Poincaré sections, and bifurcation diagram, which allows a real-time analysis of the acquired data for experimental identification of equilibrium points, periodic and chaotic attractors, and bifurcations. The experimental mapping of the circuit behavior is realized with the variation of a parameter, where a series of bifurcation is observed in its dynamical behavior.

2 Analogous Chua's circuit

There are several alternatives to implement the Chua's circuit, generally based in an electronic version of the Chua's diode combined with an inductor or an inductance emulator [10]. In this paper, the experimental characterization is realized using the analogous Chua's circuit, an inductor-free version that reproduces the dynamical behavior of the Chua's circuit with a remarkable similarity between theoretical simulations and the experimental results [7]. The three first-order differential equations that describe the Chua's circuit are emulated by analog weighted electronic integrators, which are adequately interconnected as shown in Fig. 2 in order to obtain the analogous Chua's circuit. The methodology proposed by Rocha et al. [11] is used to design this analogous circuit, which is based in the dimensionless approach of the Chua's system

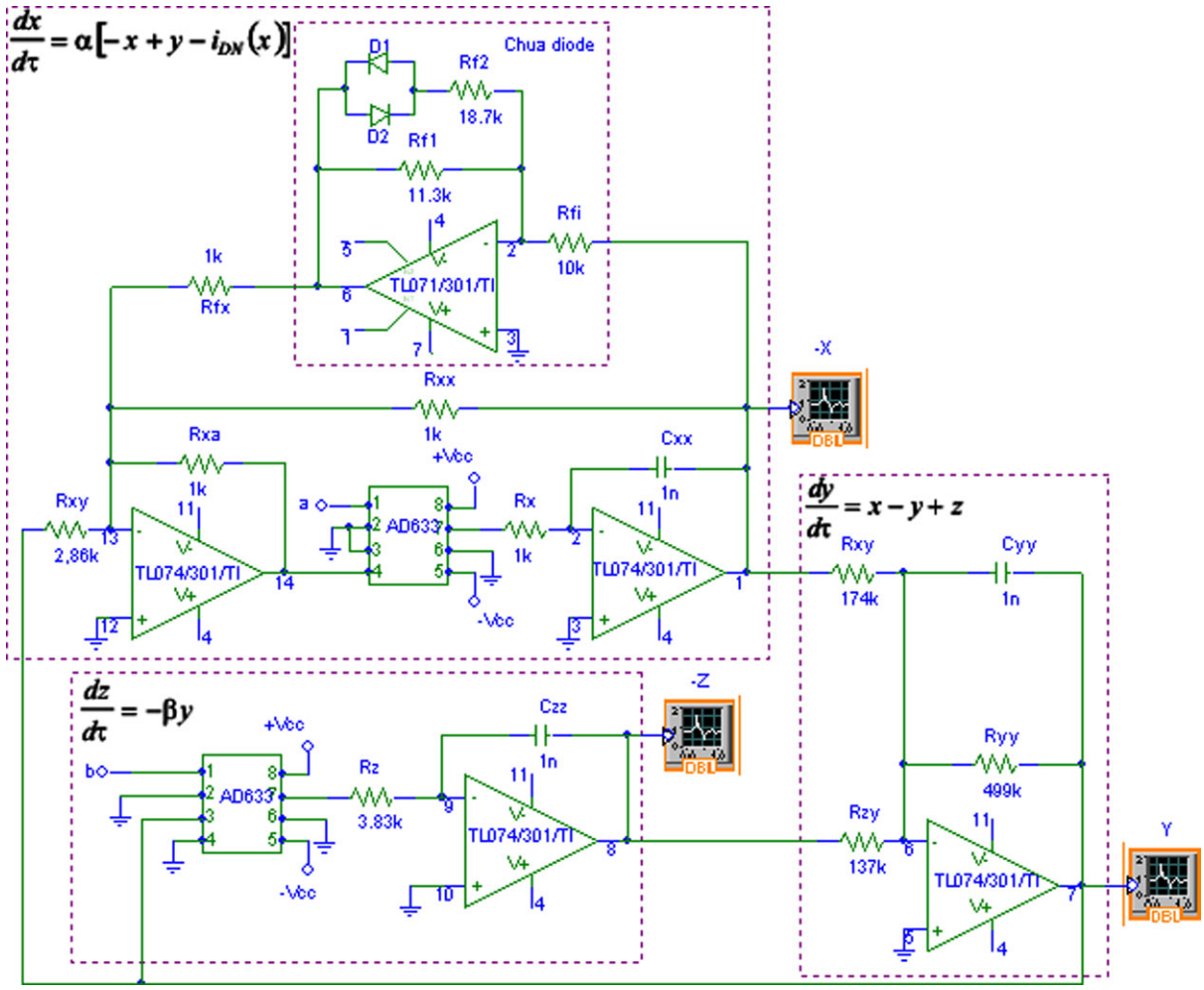

Fig. 2 Analogous Chua's circuit: the dynamic of Chua's circuit is defined by three coupled differential equations: $dx/dt = \alpha[-x + y - i_{\mathrm{DN}}(x)]$, $dy/dt = x - y + z$, and $dz/dt = -\beta y$, where $i_{\mathrm{DN}}(x)$ is the characteristic of the Chua's diode. These equations are emulated using analog weighting integrators, which are adequately interconnected to provide a versatile and functional inductorless version of the Chua's circuit. The circuit inputs are DC voltages that determine the parameter values α and β. The output signals of this circuit are $(-x)$, (y), and $(-z)$

where equivalent parameter configurations are eliminated grouping the seven original parameters R', C_1, C_2, L, m_0, m_1, and B_p into only four dimensionless groups $\alpha = C_2/C_1$, $\beta = R'^2 C_2/L$, $a_0 = R'm_0$, and $a_1 = R'm_1$. Although the number of components used to implement this analogous circuit is larger than other Chua's oscillator configurations, it offers new and interesting features for comfortable measurements using an acquisition board (DAQ). The three state variables are accessible and can be directly acquired by a DAQ, since they are explicitly available as voltage signals, which amplitudes and frequencies are independently

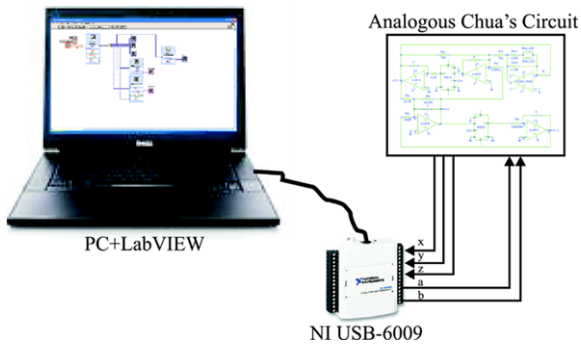

Fig. 3 Experimental apparatus for data acquisition

defined in circuit design from scaling [7]. Thus, the characteristics of the output signals of the analogous Chua's circuit can be adjusted according to DAQ specifications. Another advantage of the analogous Chua's circuit is that the parameters α and β can be easily varied in a large range by external DC voltage levels provide by the DAQ, facilitating the automatic computational analyses of the circuit. The experimental analogous Chua's circuit is implemented using the IC's AD633 (analog multiplier), IC TL071 (single op-amp) and IC TL074 (quad op-amp). Two red LEDs are used in an antiparallel diodes configuration of the analogous Chua's diode. The normalized dimensionless parameters $a = \alpha/35$ and $b = \beta/35$ are represented by external DC voltage levels. In this work, the parameter b is fixed in 3 V.

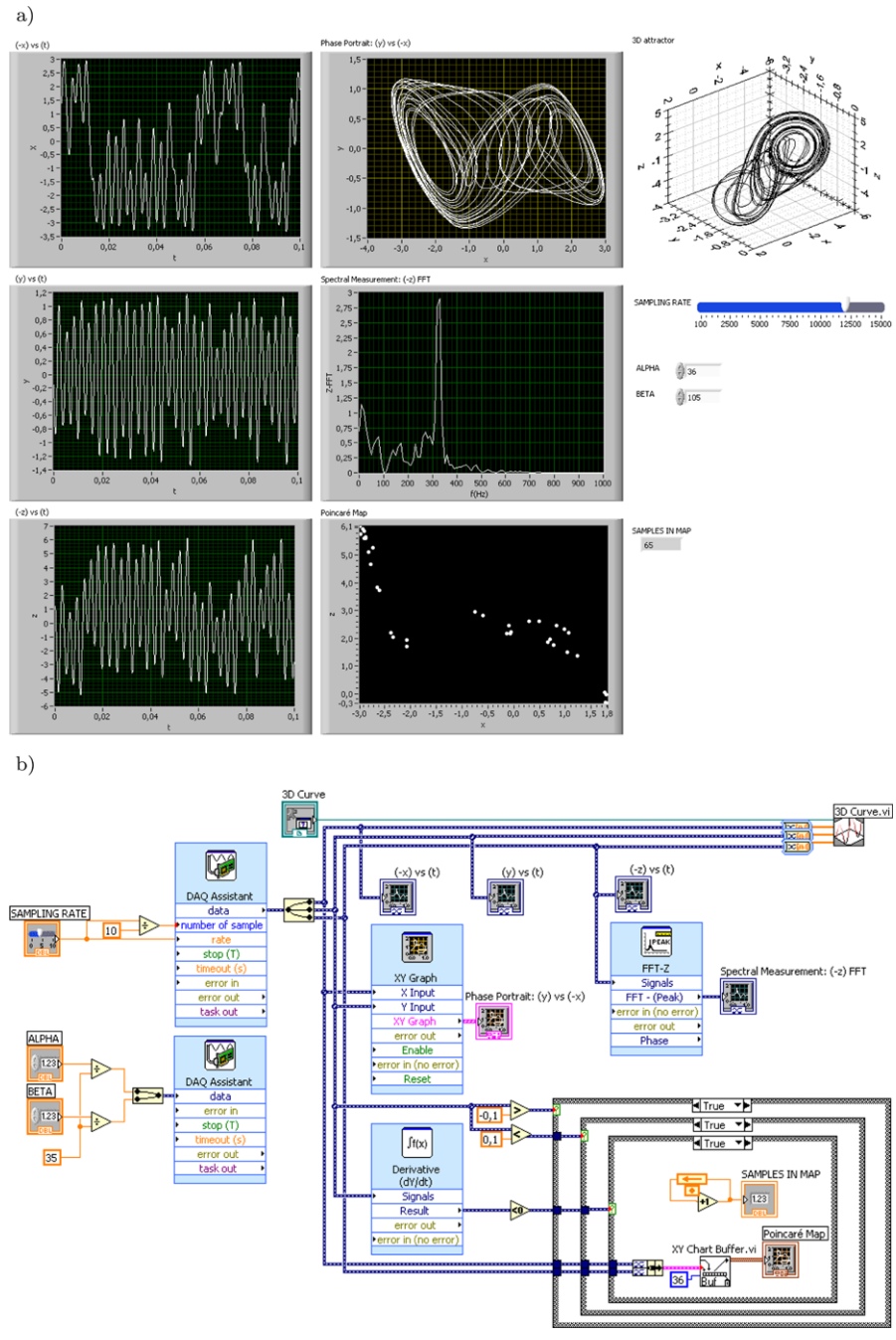

Fig. 4 LabVIEW windows. (**a**) Frontal panel: this window is the interface between the user and LabVIEW program and allows a simultaneous visualization of three time waveforms, phase portrait, 3D attractor, spectral measurements, Poincaré map and the quantity of sampled points in the Poincaré section. From this panel, the DAQ sampling rate and the parameter values can be adjusted using the controls inputs. (**b**) Block diagram: this windows has the graphical source code of the LabVIEW program, which establishes the dataflow path to execute the signal processing

3 Data acquisition

3.1 Hardware

The experimental apparatus for data acquisition and signal processing is presented in Fig. 3. The electrical signals generated by the analogous Chua's circuit are acquired at a rate of 16 kSamples/s by three single ended analog inputs of a NI USB-6009, a USB based data acquisition (DAQ) and control device manufactured by National Instruments. This DAQ has 8 referenced single ended signal coupling or 4 differential signal coupling analog inputs (14-bit resolution, 48 kSamples/s), and 2 analog outputs (12-bit resolution, 150 samples/s), which are used to generate the parameters a and b for the analogous Chua's circuit. It has still 12 configurable digital input/output (5V TTL/CMOS) and a 32-bit counter.

3.2 Software

The real-time data analysis is realized using the Laboratory Virtual Instruments Engineering Workbench (LabVIEW), which is a software widely used for data acquisition, prototyping and testing, containing a comprehensive set of tools for acquiring, analyzing, displaying, and storing data. The main concepts and techniques for LabVIEW programming can be found in manuals [12, 13]. The LabVIEW programming is visual and uses graphical representations of functions, mathematical subroutines, displays, and other utilities extremely useful for data analysis and signal processing. Since a LabVIEW program imitates physical instruments, it is called virtual instrument (VI) and presents two fundamental parts as shown in Fig. 4: the frontal panel and the block diagram.

The frontal panel is shown in Fig. 4a and consists in the interface between the user and the VI. This window is composed by controls and indicators, which are available in the "controls palette" and consist in the interactive inputs and outputs terminals of the VI, respectively. The controls are knobs, push, buttons, dials, and other elements that simulate inputs mechanisms in a VI, while the indicators are the outputs mechanisms of a VI such as graphs, charts, LEDs, and other elements for visualization of signals or alarms.

The block diagram is the graphical source code of a VI shown in Fig. 4b, which is built in a second window using terminals, nodes, and wires. The terminals are entry and exit ports that exchange information between the front panel and block diagram. Thus, for each control or indicator placed in the frontal panel, an icon terminal is inserted on the block diagram. Nodes are objects on the block diagram with inputs and/or outputs that perform operations, which can be available in the "functions palette" or created by the own user as another VI. The main types of nodes in LabVIEW are functions (statements, operators, or functions), sub-VIs (subroutines), Express VIs (sub-VIs designed to aid in common measurement tasks), and structures (repetition loops or case statements). Terminals and nodes are wired to establish the flow of data in the block diagram.

In the execution of a VI, the data inserted in the frontal panel will flow to the block diagram through the terminals. When a node receives all required inputs, it executes a function, sub-VI, or structure and

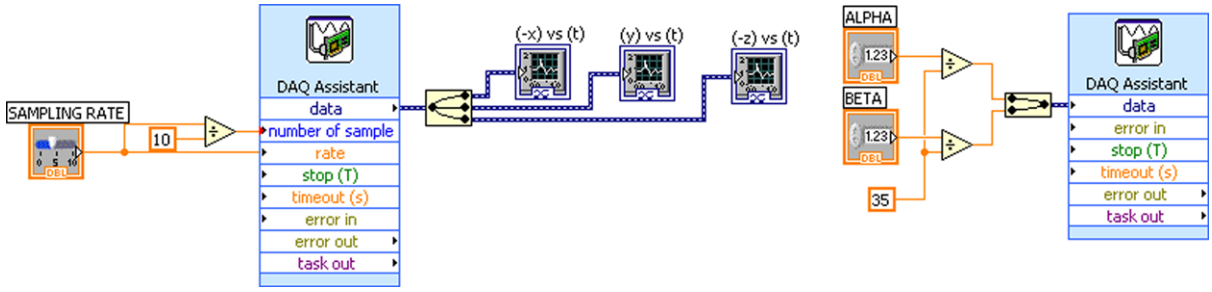

Fig. 5 LabVIEW block diagram for visualization of the waveforms $(-x)$ vs. (t), (y) vs. (t) and $(-z)$ vs. (t). The VI communicates with the DAQ using the interactive block DAQ Assistant Express VI, where the acquisition channels are configured. The input data of DAQ Assistant can be directly inserted in the frontal panel. The output of DAQ Assistant is split to recover the acquired signals x, y and z, which are exhibited in distinct waveform graphs. The analog output channels of the DAQ are configured in other DAQ Assistant to generate the DC signals that correspond to the parameters to Chua's circuit, which are directly defined in the frontal panel

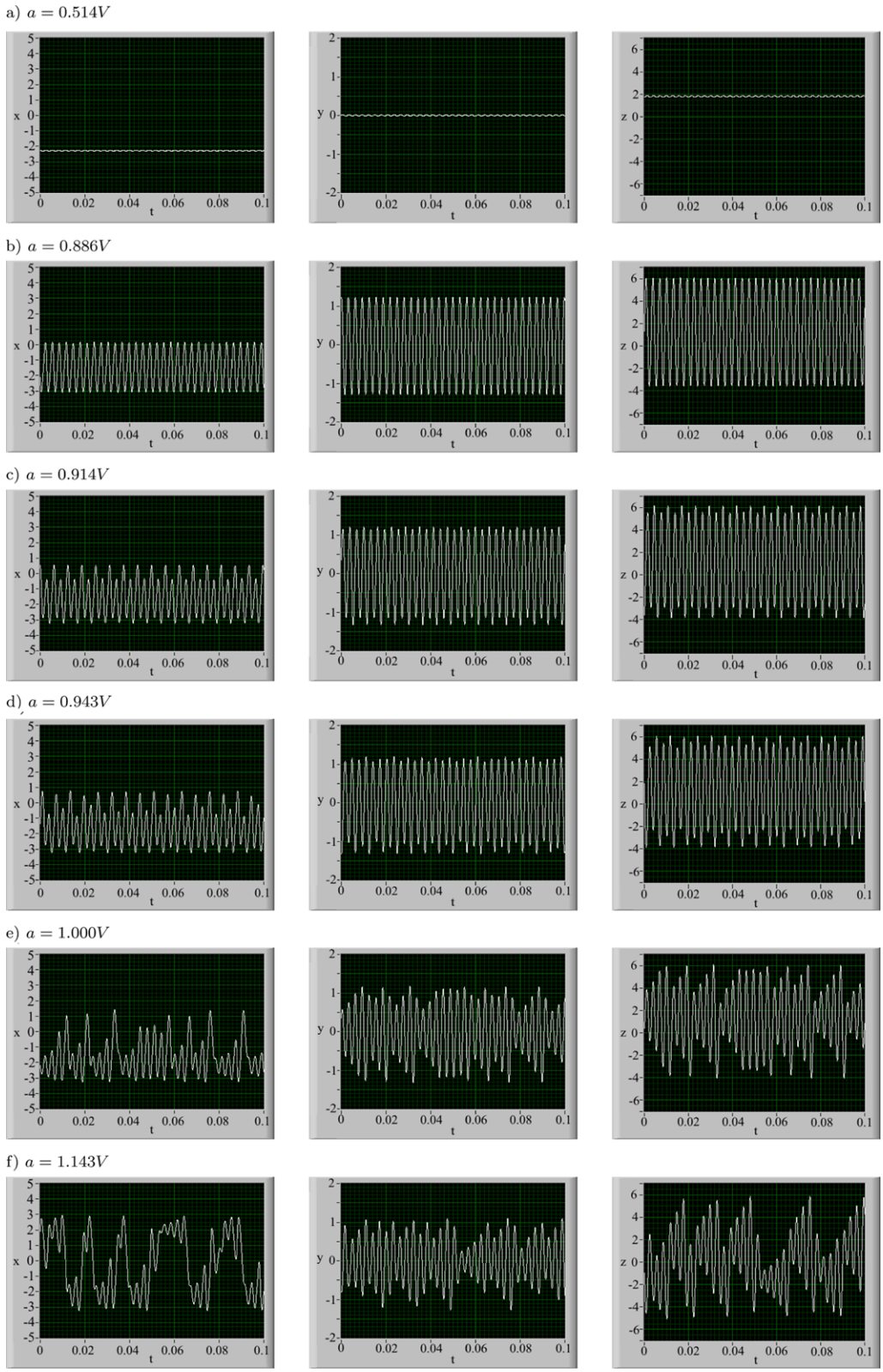

Fig. 6 Time waveforms generated in analogous Chua's circuit: $(-x)$ vs. (t), (y) vs. (t), and $(-z)$ vs. (t) are presented in the first, second and third column, respectively. The parameter a is indicated in each figure and the parameter b is always 3 V

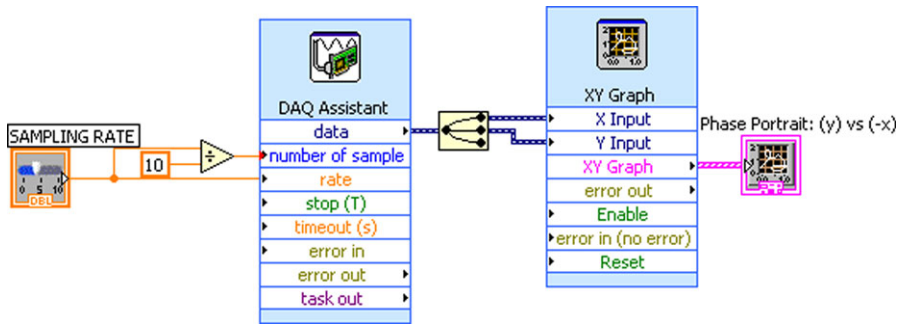

Fig. 7 LabVIEW block diagram for visualization of the phase portraits (y) vs. $(-x)$. To observe XY graphs, the signals are formatted in the "XY Graph,' an Express VI that is not located on the "functions palette" and automatically appears on the block diagram when an "XY graph" is placed on the front panel

produces output data that are passed to next node or terminal in the dataflow path, which determines the execution order of the VIs and functions on the block diagram.

4 Experimental investigation

4.1 Time waveforms

The visualization of time waveforms is normally a straightforward, direct, and trivial method for analysis of the system behavior. The time waveforms can be easily observed using oscilloscopes as a two-dimensional graph of the studied variable (vertical axis), plotted as function of time (horizontal axis). While periodic waveforms present a regular pattern, aperiodic waveforms such as those of quasi-periodicity or chaos appear to be shaking, which is generally a signature of these nonlinear phenomena. If a DAQ or a digital storage oscilloscope (DSO) is used, the waveform can be "frozen" at a certain instant and the irregular behavior of a chaotic waveform becomes apparent. The LabVIEW program to visualize the waveforms is shown in Fig. 5. The waveforms generated by analogous Chua's circuit for different values of a are presented in Fig. 6. When $a = 0.514$ V, the behavior of the circuit corresponds to an equilibrium point indicated by the constant DC time waveforms. A periodic behavior is observed for $a = 0.886$ V and $a = 0.914$ V, since all waveforms are evidently regulars. The circuit behavior for $a = 0.943$ V also seems be regular. For $a = 1.000$ V and $a = 1.143$ V, none pattern is verified in the time evolution of the variables, which can characterize the chaotic behavior.[1]

4.2 Phase portraits and attractors

The phase portrait is a geometric representation of dynamical system trajectories in the phase plane, a coordinate frame defined by independent variables that describe the system dynamics and where all possible states of a system can be represented. The phase portraits consists in an important tool for the study of dynamical systems, since its behavior is evidenced and identified, revealing information such as whether an attractor, a repeller or a limit cycle is present for a chosen parameter value. While a stationary system is represented by a point in the phase plane, a periodic system presents a closed orbit (limit cycle). A chaotic behavior is characterized by phase portraits that present a region where the trajectories are always describing different orbits. The phase portraits of random noise is easily identified by fuzzy edges. The 2D phase portraits can be displayed in an oscilloscope using the X–Y mode instead of a sweeping time base. For the visualization of the phase portraits, the block "Build XY Graph" is included in the LabVIEW programming as shown in Fig. 7. The series of phase portraits presented in Fig. 8 show how the behavior of the analogous Chua's circuit evolutes from an equilibrium point to a chaotic motion when the parameter a varies from 0.514 V to 1.371 V. For $a \leq 0.514$ V, it is observed an equilibrium point. The behavior is

[1] One can also identify the chaotic nature of the signal by looking at the random-like variation of the amplitude signal.

periodic with period-1 (1 revolution) in the interval $0.760\ \text{V} \leq a \leq 0.886\ \text{V}$ and period-2 (2 revolution) at $a = 0.914$ V. When $a = 0.943$ V, the dynamical behavior of the circuit becomes apparently chaotic. The behavior is a Rössler-type attractor in the interval of $0.971\ \text{V} \leq a \leq 1.000$ V. In the range $1.029\ \text{V} \leq a \leq 1.371$ V, there is another chaotic attractor called double scroll. Embedding this region, there is a window of periodic behavior at $a = 1.171$ V. For $a > 1.371$ V, the system is unstable. The LabVIEW allows to visualize the 3D phase portrait using the block "3D curve," as shown Fig. 9. The complete 3D phase portraits of the analogous Chua's circuit for $0.514\ \text{V} \leq a \leq 1.371$ can be seen in Fig. 10.

4.3 Frequency spectra

The spectral methods are the most used tools for signal analysis. Since any waveform can be represented

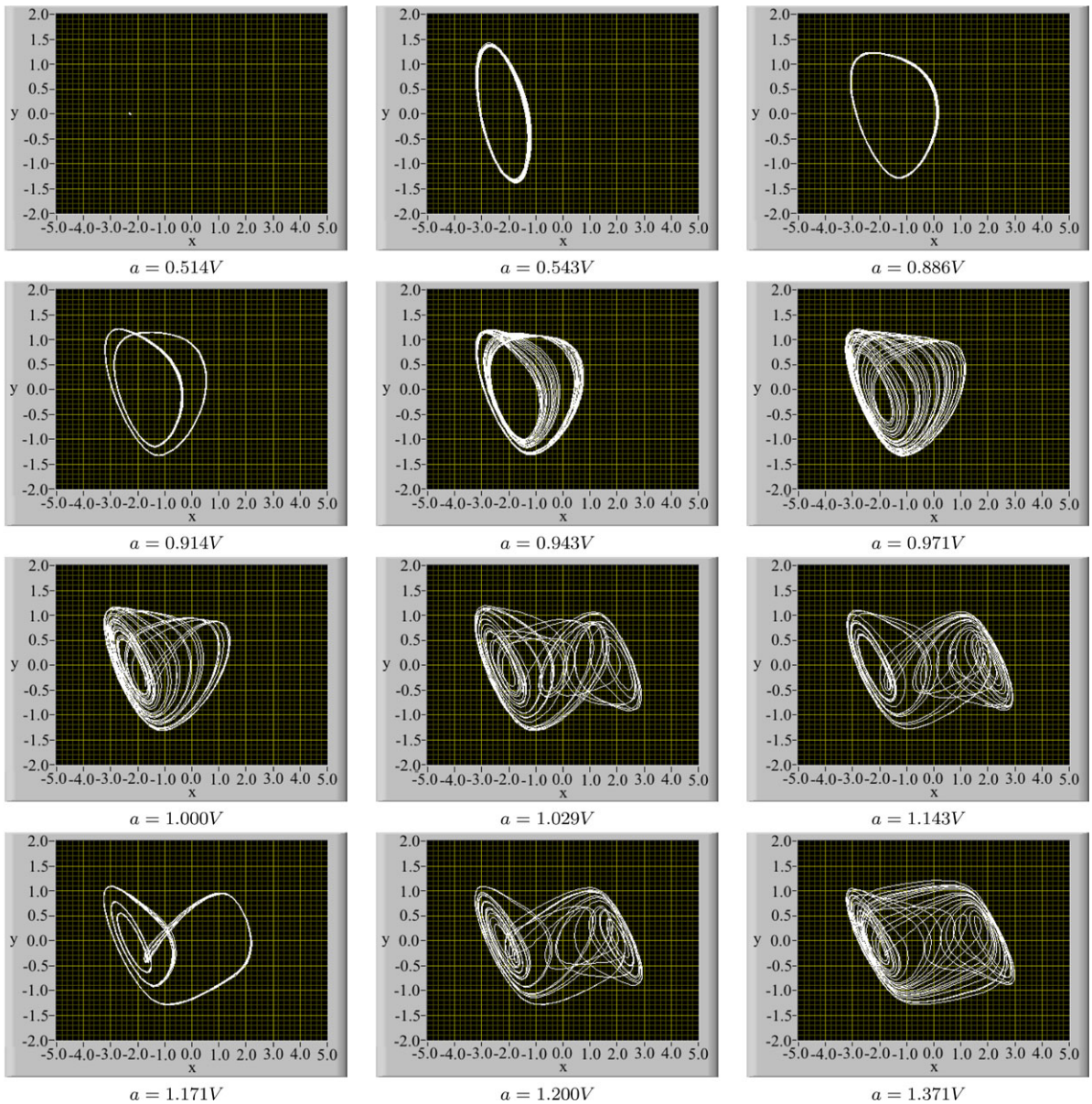

Fig. 8 2D phase portraits $(-x)$ vs.. (y): dynamical behavior of the analogous Chua's circuit for $0.514\ \text{V} \leq a \leq 1.371$ V and $b = 3$ V

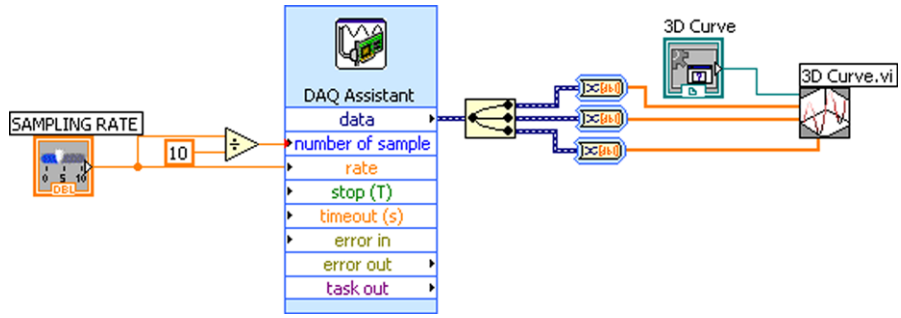

Fig. 9 LabVIEW block diagram for visualization of the three dimensional attractors. The acquired signals are converted into an appropriate format to be described in terms of lines in 3D space by the block "3D Curve.vi" and plotted in a 3D graph using the terminal "3D Curve"

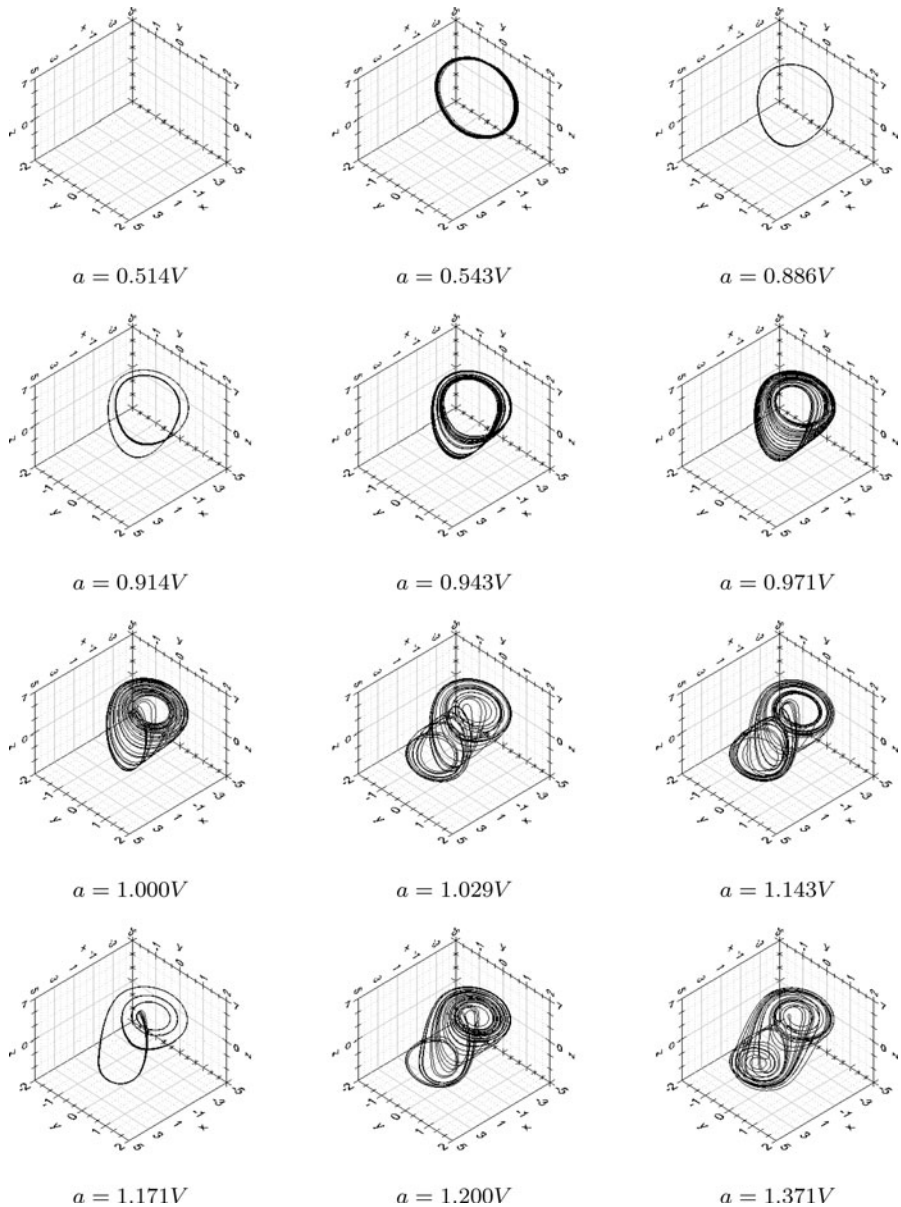

Fig. 10 3D phase portraits: dynamical behavior of the analogous Chua's circuit for $0.514\ \text{V} \leq a \leq 1.371\ \text{V}$ and $b = 3\ \text{V}$

by the summation of an unique combination of sine waves, the magnitude and phase evaluation of each sinusoidal component of the wave provides important information about the nature of a system. Since only a nonlinear behavior introduces new frequencies in the spectrum, the spectral analysis can be used to identify nonlinear systems. The spectral analysis also allows to distinguish periodic, chaotic, and stochastic behaviors: while the noises present a random frequency spectrum, the chaotic signals are wide-band signals, and both can be easily distinguished from periodic signals that presents only stable frequencies. The magnitude and phase of each frequency component are obtained from the Fourier transform, which can be approximately computed using an algorithm so-called Fast Fourier transform (FFT). Spectrum analyzers and some digital storage oscilloscopes use the FFT algorithm to realize a direct spectral analysis of real signals. In the LabVIEW environment, the block diagram to obtain the graph of the frequency spectrum is shown in Fig. 11. For the analogous Chua's circuit, the spectral graphs of the $(-z)$ signal are presented in Fig. 12, where can be observed the evolution of its behavior. The spectrum for $a = 0.514$ V presents a only peak in 0 Hz, which means that the $(-z)$ time waveform is a DC offset and the circuit dynamics is an equilibrium point. For $a = 0.760$ V, the circuit behaves as a linear system operating as sinusoidal oscillator, since a single nonzero frequency appears in the spectrum. A periodic nonlinear behavior is clearly characterized for $0.886\ \text{V} \leq a \leq 0.943\ \text{V}$ due to well defined frequencies in the spectrum of the measured signal. Although the behavior of the circuit for $a = 0.943$ V has not been accurately determined in the previous analyses, the spectral analysis shows that it is definitively periodic. For $0.971 \leq a \leq 1.371$, the frequencies are not well defined and occupy a wide band of the spectrum, which characterizes the chaotic behavior, except at $a = 1.171$ V, where the well-defined frequencies in the spectrum indicate a periodic window.

4.4 Poincaré section

From a two-dimensional projection of an attractor, a periodic orbit can be confidently identified for the most cases. However, this approach does not allow usually a definitive conclusion between quasi-periodic and chaotic attractors. A better resolution is given by the analysis of the Poincaré section, a two-dimensional plane that intersects the steady-state trajectories, as shown Fig. 13, and converts a continuous flow into a discrete-time mapping (Poincaré map). By definition, only one direction of crossing of the trajectory must be considered. Observing the stroboscopic distribution of the discrete points on the Poincaré section, it is possible to identify the behavior of the system. For a periodic motion, it is observed a finite number of points on the Poincaré section that adequately reflect the periodicity of the motion. A continuous line in the Poincaré map is observed for a quasi-periodic motion. If the motion is chaotic, it is verified a large number of irregularly and densely located points on the plane due to the fractal nature of the chaotic attractors. Although its experimental observation may appear nontrivial, techniques for visualization of the Poincaré section using an oscilloscope can be found in the bibliography [9].

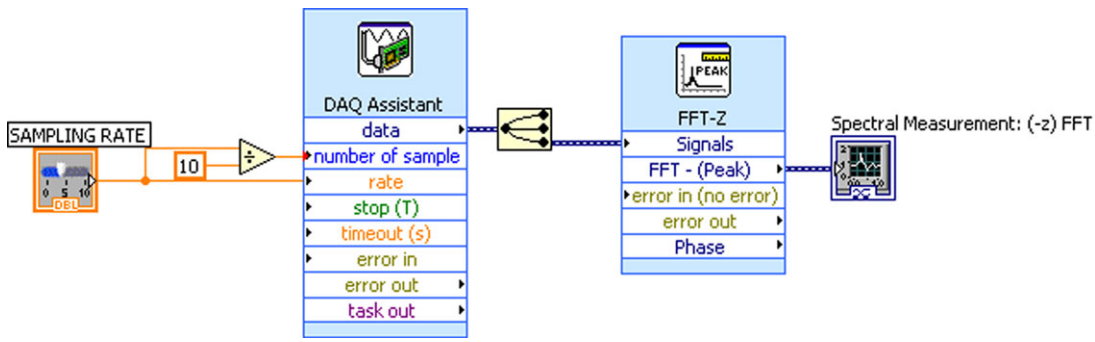

Fig. 11 LabVIEW block diagram for spectral analysis. The block "Spectral Measurements" (FFT-Z) performs the FFT-based spectral measurements (averaged magnitude spectrum, power spectrum, or phase spectrum) on acquired signals $(-z)$, assuming that a finite block of signal data represents one period of a periodic signal. In this VI, the block "Spectral Measurements" was configured to return the root-mean-square (RMS) values of the magnitude spectrum

For the visualization of a Poincaré section using the LabVIEW, the block "XY Chart Buffer" is used for storage and plotting of the values of $(-x)$ and $(-z)$, as shown in Fig. 14. Considering the plane $(y) = 0$, the Poincaré map is obtained by trajectories that cross the Poincaré section from $(y) > 0$ to $(y) < 0$. The Poincaré maps of the analogous Chua's circuit are shown in Fig. 15. For $a = 0.514$ V, the trajectory converges to an equilibrium point. The attractor always hits the section in the same point for $0.760\ \text{V} \leq a \leq 0.886$ V (little variations can be explained by noises), which characterizes a periodic behavior with period-1. Note that this case (period-1) is different from the fixed point for $a = 0.514$ V, where the trajectory is always in the Poincaré section and corresponds to the steady state of the system. For $a = 0.914$ V, the attractor hits the section in two points, which means a periodic behavior with period-2, increasing the num-

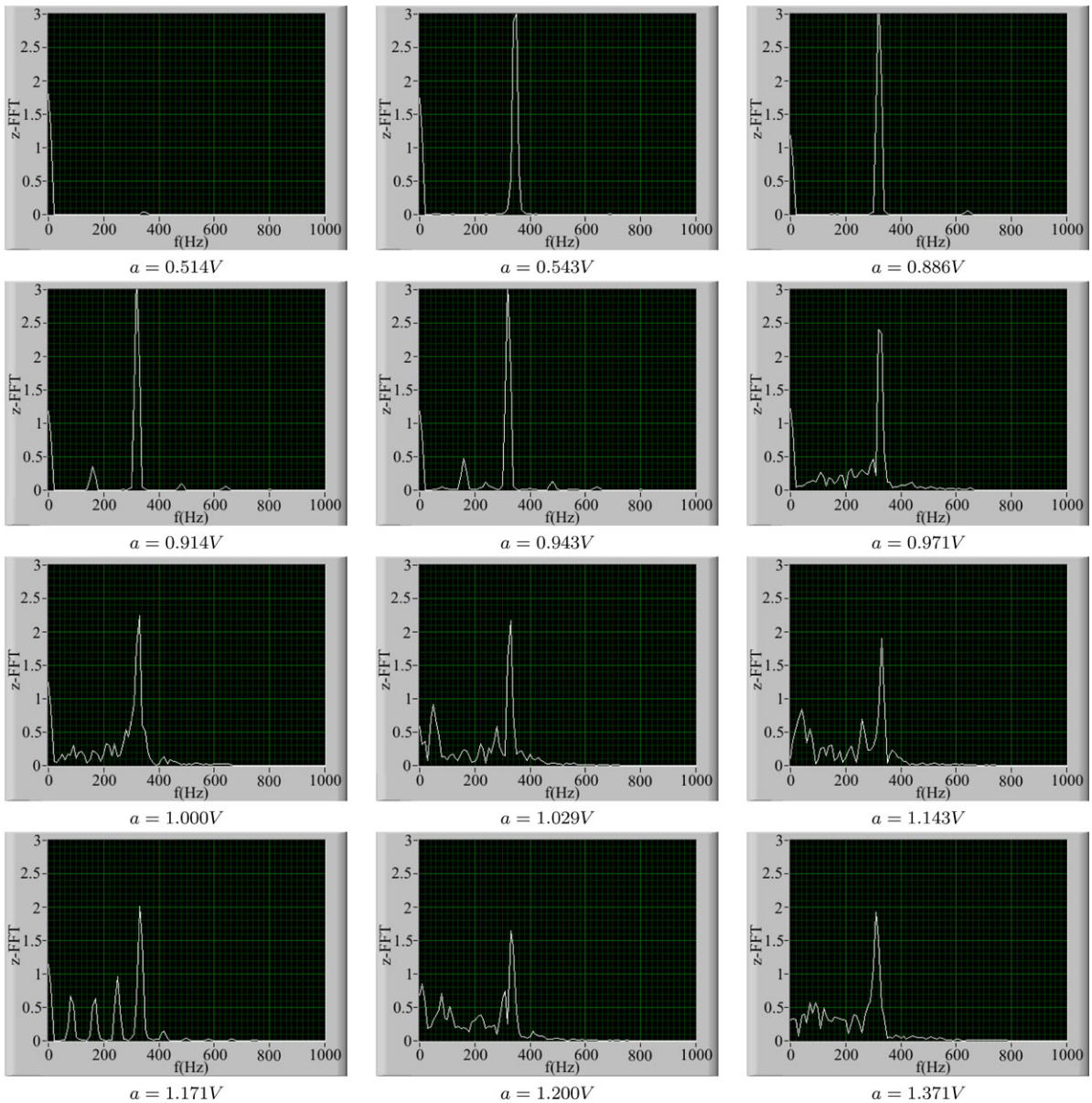

Fig. 12 Frequency spectra of $(-z)$ signal for $0.514\ \text{V} \leq a \leq 1.371$ V and $b = 3$ V

ber of the orbits until $a = 0.943$ V. Since the Poincaré map presents several different points which are irregularly distributed, the behavior of the circuit can be considered chaotic for $0.971\ \text{V} \leq a \leq 1.371$ V, except at $a = 1.171$ V. In this point, the Poincaré map indicates a periodic behavior.

4.5 Bifurcation diagrams

Since the qualitative dynamical behavior of a system changes with the parameter variations, a global description of the system involves the knowledge of all possible behaviors for several parameter values.

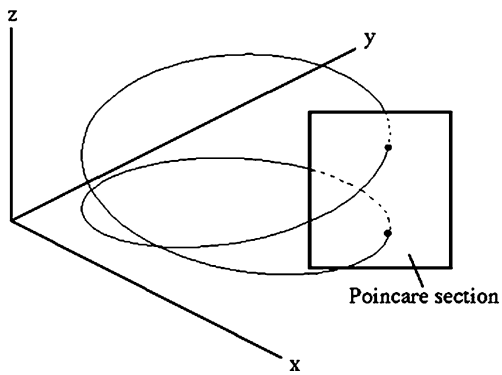

Fig. 13 Poincaré section [9]

A convenient way of displaying the variety of behaviors exhibited by a system is the bifurcation diagram, a graphical representation that shows the possible long-term values (equilibrium points, periodic orbits, chaotic orbits) of a system as function of a control parameter. A bifurcation diagram consists basically in a visual summary of the values of a determined system variable when the asymptotic behavior is reached and the trajectory hits in the Poincaré section, considering a continuous variation of the control parameter. It allows an qualitative identification of the system's behavior and its changes (bifurcation points) when some chosen parameter is varied. In a typical bifurcation diagram, the control parameter is placed in the horizontal axis and the vertical axis corresponds to the sampled variable. After discard the initial transients, a large number of samples of a system variable must be captured for each control parameter value, and plotted in the bifurcation diagram. This sampling is realized using a Poincaré section. An extra electronic circuit is required aiming to display an experimental bifurcation diagram using an oscilloscope [9]. Here, the experimental bifurcation diagram is obtained using the LabVIEW environment (see the block diagram in Fig. 16). When a sufficient quantity of points of the system variable is sampled in a Poincaré section ($(y) = 0$), the control parameter is automatically incremented. The experimental bifurca-

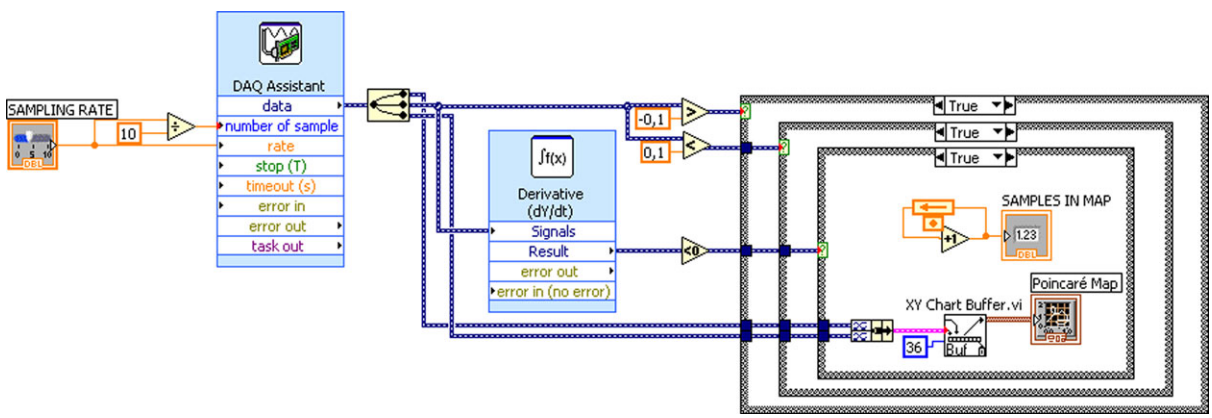

Fig. 14 LabVIEW block diagram to plot a Poincaré map. To detect when a trajectory hits in the Poincaré section $(y) = 0$, two conditions are tested using case structures: $(y) > -\epsilon$ and $(y) < \epsilon$. The more inner case structure verifies the condition $d(y)/dt < 0$ to determine if the trajectory crosses the Poincaré section in direction positive to negative (y). The time derivative of the (y) signal is computed using the "Time Domain Math" block (Derivative dY/dt). When all these conditions are true, the $(-x)$ and $(-z)$ signals are sampled, stored in "XY Chart Buffer.vi" and plotted in a chart. The block "XY Chart Buffer.vi" stores a fixed quantity of data (36 points), updating the more old points by new points when the buffer is full. The quantity of sampled points is counted and displayed in the frontal panel

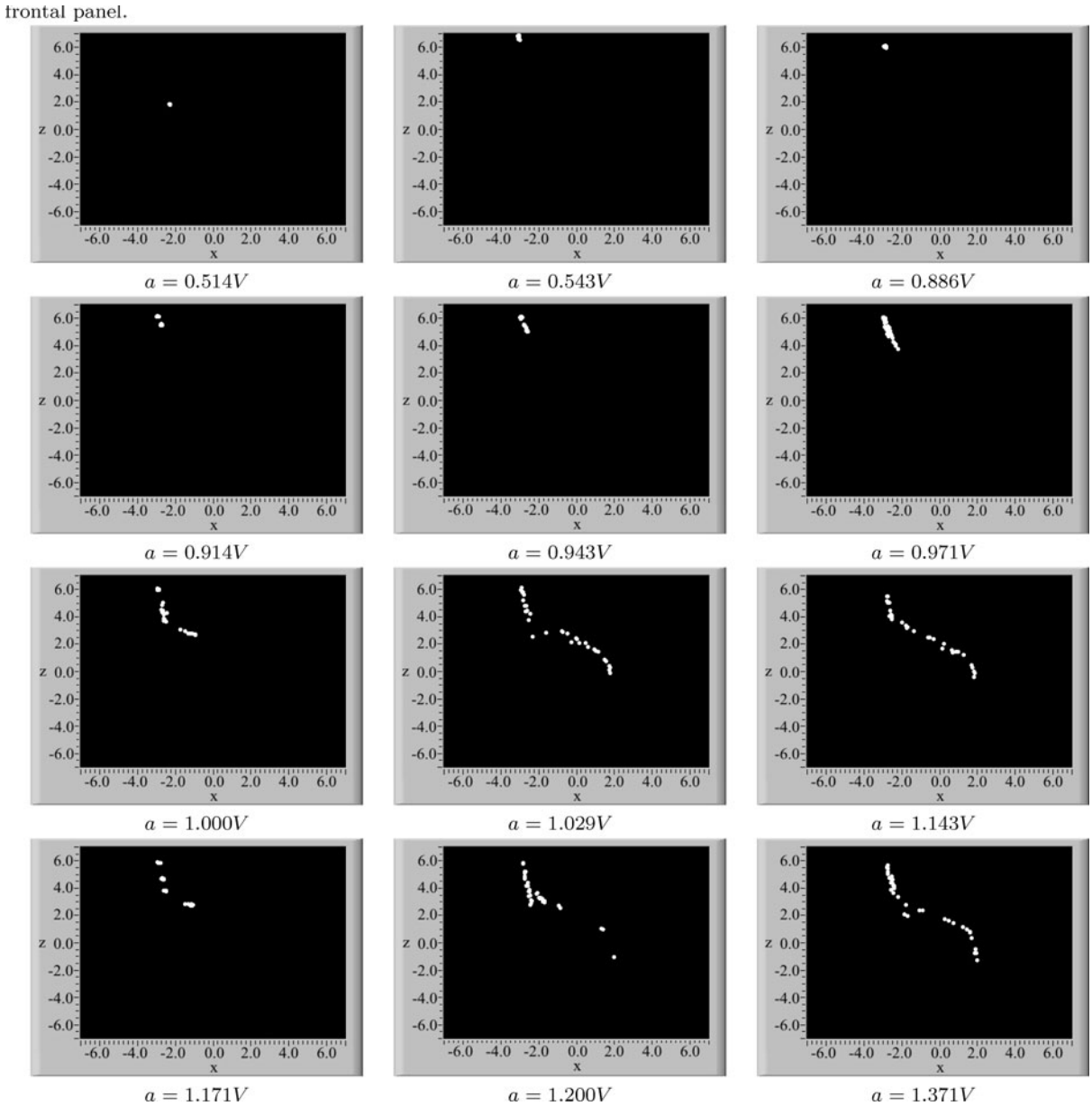

Fig. 15 Poincaré maps in the section $(y) = 0$ for 0.514 V $\leq a \leq$ 1.371 V and $b = 3$ V

tion diagram $(-z)$ vs. a for the analogous Chua's circuit is presented in Fig. 17, where the control parameter a varies from 0.085 V to 1.371 V. The conventional route to chaos by period doubling is observed, where the circuit behavior is an equilibrium point until $a \approx 0.514$ V, becoming periodic with period-1 until $a \approx 0.914$ V, when the periodic behavior bifurcates to period-2, period-4, and period-8, until finally reaches the chaos at $a \approx 0.971$ V.

5 Conclusions

The behavior of the analogous version of the Chua's circuit proposed by Rocha and Medrano [7] is experimentally characterized using usual laboratories techniques for investigation of nonlinear phenomena. These techniques, normally based in the use of oscilloscopes and sophisticated measurement equipments, are adapted to LabVIEW, which provides an adequate

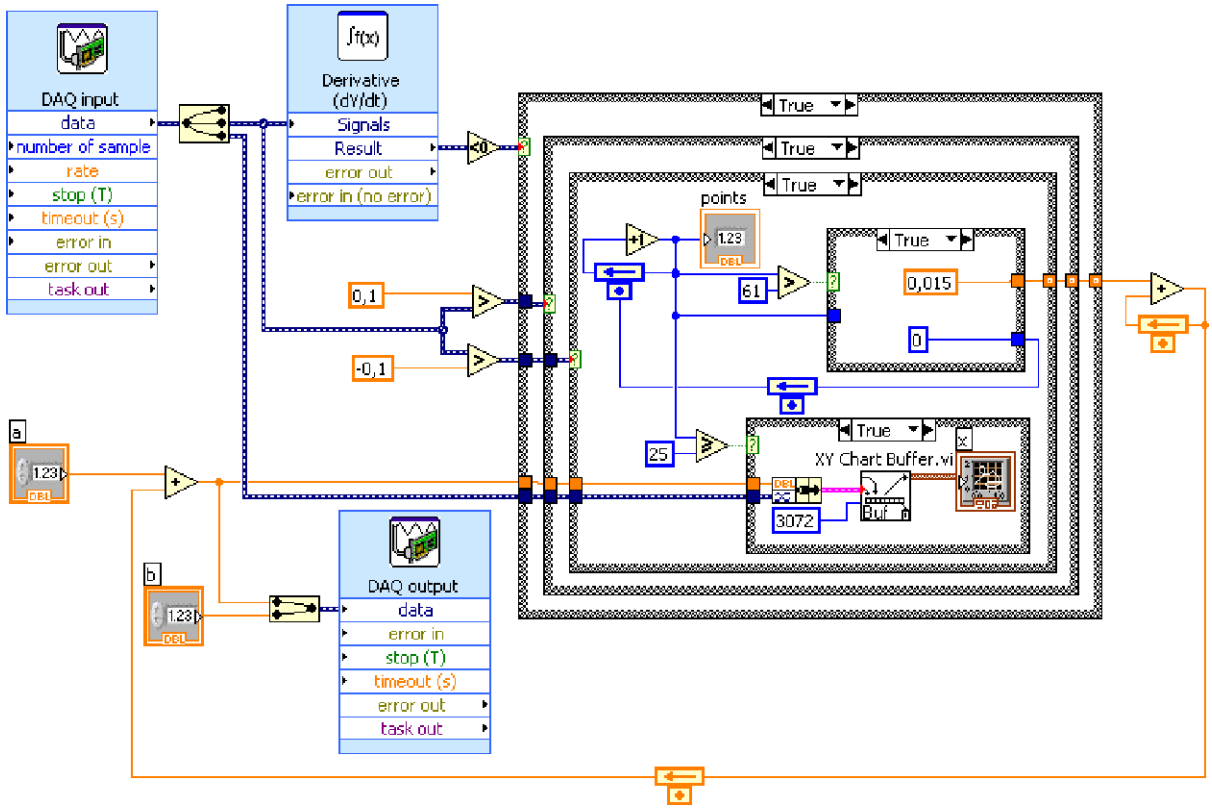

Fig. 16 LabVIEW block diagram for plotting of the bifurcation diagram. Three conditions are tested using case structures to verify when the trajectory hits in the Poincaré section $(y) = 0$: $(y) > -\epsilon$, $(y) < \epsilon$ and $d(y)/dt < 0$. If all these conditions are true, the $(-z)$ signal and the control parameter a are sampled and counted. The sampled points are stored in "XY Chart Buffer.vi" and plotted in a chart after discard the initial samples (25 points). When a determined number of samples (61 points) of the $(-z)$ signal for the same control parameter a are reached, the control parameter is incremented and the counter is reset to begin a new sampling cycle. When the buffer is full, the bifurcation diagram will exhibit 3,072 points, and the more old points will be updated by new points

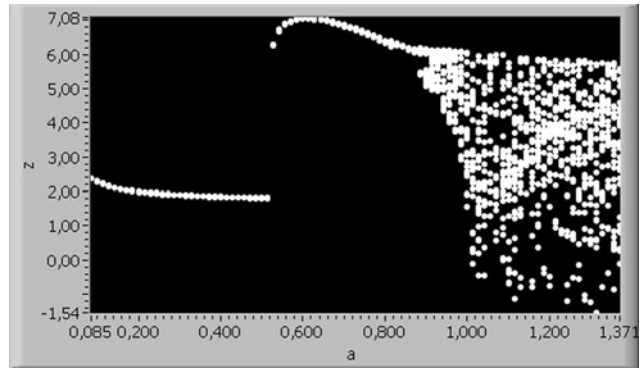

Fig. 17 Experimental bifurcation map for $0.085\ \text{V} \leq a \leq 1.371\ \text{V}$ and $b = 3\ \text{V}$

environment for the analysis of the time series captured from experimental implementations by a data acquisition system (DAQ). Time waveforms, phase portraits, frequency spectra, Poincaré sections, and bifurcation diagrams can be simultaneously observed in a low expensive LabVIEW-based platform, allowing a real-time identification of equilibrium points, periodic and chaotic attractors, and bifurcations. Thus, the be-

havior of the circuit is experimentally mapped considering the variation of a parameter, where is observed the route to chaos by period doubling, a characteristic of the Chua's circuits. Considering the versatility of the analogous Chua's circuit, this experimental platform can be used to investigate other characteristics of the nonlinear systems and new bifurcation phenomena. This work also contributes for the development of experimental activities for study of other real systems, since the presented platform consists in an attractive and low expensive tool for data acquisition of times series and real-time analysis of nonlinear phenomena if compared with conventional laboratory techniques using oscilloscopes and sophisticated measurement equipments.

Acknowledgements The authors gratefully acknowledge National Counsel of Technological and Scientific Development (CNPq), State of Minas Gerais Research Foundation (FAPEMIG), State of São Paulo Research Foundation (FAPESP), and Gorceix Foundation that contributed to the development of this project.

References

1. Ditto, W., Munakata, T.: Principles and applications of chaotic systems. Commun. ACM **38**, 96–102 (1995)
2. Yang, S.-K., Chen, C.-L., Yau, H.-T.: Control of chaos in Lorenz system. Chaos Solitons Fractals **13**, 767–780 (2002)
3. Cuomo, K.M., Oppenheim, A.V., Strogatz, S.H.: Synchronization of Lorenz-based chaotic circuits with applications to communications. IEEE Trans. Circuits Syst. II **40**, 626–633 (1993)
4. Madan, R.N.: Chua's Circuit: A Paradigm for Chaos. World Scientific, Singapore (1993)
5. Medrano-T, R.O., Baptista, M.S., Caldas, I.L.: Basic structures of the Shilnikov homoclinic bifurcation scenario. Chaos **15**, 33112 (2005)
6. Albuquerque, H.A., Rubinger, R.M., Rech, P.C.: Self-similar structures in a 2D parameter-space of an inductorless Chua's circuit. Phys. Lett. A **372**, 4793–4798 (2008)
7. Rocha, R., Medrano-T, R.: An inductor-free realization of the Chua's circuit based on electronic analogy. Nonlinear Dyn. **56**, 389–400 (2009)
8. Suneel, M.: Electronic circuit realization of the logistic map. Sadhana **31**, 69–78 (2006)
9. Tse, C.: Experimental techniques for investigating chaos in electronics. In: Chaos in Circuits and Systems, Chap. 18, pp. 367–384. World Scientific, Singapore (2002)
10. Kiliç, R.: A comparative study on realization of Chua's circuit: hybrid realizations of Chua's circuit combining the circuit topologies proposed for Chua's diode and inductor elements. Int. J. Bifurc. Chaos Appl. Sci. Eng. **13**, 1475–1493 (2003)
11. Rocha, R., Martins Filho, L.S., Machado, R.F.: A methodology for teaching of dynamical systems using analogous electronic circuits. Int. J. Electr. Eng. Educ. **43**, 334–345 (2006)
12. National Instruments: Getting started with LabVIEW (2007)
13. National Instruments: LabVIEW fundamentals (2007)